

Velocity distributions in dilute granular systems

J. S. van Zon^{1,2,*} and F. C. MacKintosh^{1,2,†}

¹*Division of Physics and Astronomy, Vrije Universiteit, 1081 HV Amsterdam, The Netherlands*

²*Institute for Theoretical Physics, University of California, Santa Barbara, CA 93106*

(Dated: December 2, 2024)

Motivated by recent experiments reporting non-Gaussian velocity distributions in driven dilute granular materials, we study by numerical simulation the properties of inelastic gases as functions of the coefficient of restitution η and concentration ϕ with various heating mechanisms. We show that there are marked, qualitative differences in the behavior for uniform heating (as is frequently assumed theoretically) and for particle systems driven at the boundaries of the container (as is frequently done in experiments). We find non-Gaussian (*stretched* Gaussian) behavior of the form $\exp[-\beta v^\alpha]$ for velocities larger than the rms velocity, with a range of exponents $0.7 \lesssim \alpha \leq 2$. For smaller velocities, we consistently find a crossover to nearly Gaussian behavior. Thus, we do not find a universal value of $\alpha = 3/2$, as suggested by recent experiments and as predicted by kinetic theories. Moreover, we demonstrate that very similar behavior is found for a simple model of a gas of particles with no spatial degrees of freedom.

PACS numbers:

I. INTRODUCTION

Granular materials consisting of macroscopic particles or grains can exhibit behavior reminiscent of conventional phases of matter. Sand, for instance, can flow like a liquid under some conditions. Dilute granular systems, or *gases*, have been extensively studied both experimentally and theoretically, in large part as simple model systems exhibiting nonequilibrium and dissipative behavior. These systems are intrinsically dissipative and out of equilibrium, even though it is tempting to apply such equilibrium notions as temperature. Since the collisions in such a gas are inelastic, it is necessary to supply energy, or to drive them in order to maintain a gas-like steady state. Otherwise, *inelastic collapse* can occur, in which all motion ceases after only a finite time[1, 2]. In principle, it is possible to heat or drive the system uniformly throughout the container (*uniform heating*), as has been done in simulations[3, 4], and as is assumed in many analytic theories[5]. In experiments, however, one usually drives a granular gas by shaking or vibrating the walls of the container. Such *boundary heating* means that the energy is inserted in a spatially inhomogeneous way[6, 7, 8, 9]. As a consequence, the gas will develop a gradient in density and mean kinetic energy. Even for uniform heating, however, significant deviations from equilibrium gases, e.g., in density correlations, are observed[3]. It is often assumed that in the bulk, where the boundaries are far away and spatial gradients are small on the scale of the mean free path of the particles, both heating methods should give the same results for velocity distributions. Here, we show that there are striking differences in the behavior of driven granular gases depending on whether

the heating is spatially homogeneous or not, even in the bulk and away from boundaries.

There has been much interest recently in another aspect of these non-equilibrium gases: namely, the velocity distributions. This is in part because they deviate from the Gaussian distributions that one would expect if the collisions were elastic. It has been suggested that the velocity distributions can be described by a sort-of *stretched* Gaussian, of the form $P(v) = C \exp[-\beta(v/\sigma)^\alpha]$, where $\sigma = \langle v^2 \rangle^{1/2}$ is sometimes called the granular temperature. Rouyer and Menon [8] have reported such a distribution with exponent $\alpha = 1.5$ over the whole observed range of velocities, which was unaffected by changes in amplitude and frequency of driving. This observation was particularly intriguing, given the theoretical predictions obtained before by Van Noije and Ernst [5]. They developed a kinetic theory that predicts a high-velocity tail described by a distribution with an exponent $\alpha = \frac{3}{2}$.

Unfortunately, results for velocity distributions are never unambiguous. Both in simulation and experiment, different setups and driving mechanisms usually give different behavior of the velocity distribution. For a setup where particles on a horizontal plate were driven in the vertical direction, Olafsen and Urbach [10] found a crossover from exponential to Gaussian distributions as the amplitude of the driving was increased. The result of Rouyer and Menon [8] was obtained for a different configuration where particles were confined between two vertical plates and driven in the vertical direction. Although the exponent $\alpha = 1.5$ they find is reminiscent of theoretical results obtained by Van Noije and Ernst [5], both results are actually inconsistent in that the exponent $\alpha = \frac{3}{2}$ can only describe the high-velocity tail of the distribution. Such a high-velocity tail was actually obtained by Moon et al. [4]. Using a simulation with a somewhat artificial heating mechanism they find a velocity distribution that has an exponent of $\alpha = 2.0$ for low velocities, but crosses over to an exponent of $\alpha = 1.5$ for

*Electronic address: jvzon@nat.vu.nl

†Electronic address: fcm@nat.vu.nl

the high-velocity tail. The results of Rouyer and Menon are also limited in the sense that they were obtained for almost elastic particles with $\eta = 0.93$. Blair and Kudrolli [9] use a different setup where particles move along an inclined plane. Friction with the plane during collisions reduces the coefficient of restitution to $\eta \approx 0.5$. They find the distribution with exponent $\alpha = 1.5$ only in the very dilute case. Otherwise, the distributions deviate strongly from both Gaussian and the distribution obtained by Rouyer and Menon. It is interesting to notice that for the denser case Blair and Kudrolli find a distribution with a crossover much like the type observed by Moon et al.

At present there is no agreement on what the velocity distribution of a granular gas looks like exactly nor is it clear what causes the velocity distributions to deviate from a Gaussian. Puglisi et al. [11] have suggested that the deviations are caused by the spatial correlations in the gas. They propose that for a region of uniform density the velocity distribution of the gas actually is Gaussian, with a density dependent width. The spatial correlations cause density fluctuations and they claim that the non-Gaussian distributions arise as an average over the velocity distributions over these regions of different density. It is true that an average over Gaussian distributions with different widths in general yields a stretched Gaussian, but experiments performed by Olafsen and Urbach [10] showed that this does not happen in granular gases. They find that even within small windows of uniform density the velocity distributions remained non-Gaussian. Here, we show that non-Gaussian behavior arises even in a simple model with no spatial degrees of freedom.

We study behavior of the velocity distributions of the granular gas as a function of ϕ , the area fraction, and η , the coefficient of restitution. Specifically, we consider the effect on the velocity distribution of driving the gas in a spatially homogeneous way, by uniform heating, or in a spatially inhomogeneous way, focusing mainly on boundary heating. We will show that there exists clear qualitative difference between the velocity distributions for spatially homogeneous and inhomogeneous heating. Furthermore, we will show that there is no evidence for a universal velocity distribution with a constant exponent $\alpha = 1.5$. Instead, for inhomogeneous heating, we find that velocity distributions cross over from one exponent to another for the high-velocity tail. For this high-velocity tail we observe a wide range of exponents and we find $\alpha = 1.5$ only for specific values of ϕ and η . We also present a simple model of an inelastic gas, in which no spatial degrees of freedom are included. Both in simulation and in this model we find strong evidence that the non-Gaussian velocity distributions are not caused by spatial correlations within the gas. Instead, they find their origin in the way the energy that is inserted into the system by heating, and is distributed through the gas by the inelastic collisions.

II. NUMERICAL SIMULATION

We use an event-driven algorithm to simulate N particles of radius r moving in a two-dimensional box. Particles gain energy by heating and lose energy through inelastic collisions. When two particles i and j collide their final velocities depend on their initial velocities in the following way:

$$\mathbf{v}'_i = \mathbf{v}_i - \frac{1+\eta}{2}(\mathbf{v}_i \cdot \hat{\mathbf{r}}_{ij} - \mathbf{v}_j \cdot \hat{\mathbf{r}}_{ij})\hat{\mathbf{r}}_{ij}, \quad (1)$$

where η is the coefficient of restitution and $\hat{\mathbf{r}}_{ij}$ is the unit vector connecting the centers of particles i and j .

For uniform heating we adapted an one-dimensional algorithm described in [3]. When heating uniformly, each individual particle is heated by adding a random amount to the velocity of each particle during a time step Δt :

$$\mathbf{v}_i(t + \Delta t) = \mathbf{v}_i + \sqrt{h\Delta t}\mathbf{f}(t), \quad (2)$$

where $\mathbf{f}(t)$ is a vector whose components are uniformly distributed between $-\frac{1}{2}$ and $\frac{1}{2}$ and h is proportional to the heating rate. After heating the system is transferred to the center-of-mass frame. Particles move in a box with sides $L = 2$. We use periodic boundary conditions to simulate bulk behavior. The time step Δt is chosen in such a way that on average the number of collisions per time step is less than one.

When heating through the boundaries, particles gain velocity upon collision with the boundary. For simplicity, we assume that the collision with the boundary is elastic. In that case, a collision occurs by reflecting \mathbf{v}_\perp , the component of the velocity perpendicular to the boundary. Heating occurs by adding a random amount of velocity to \mathbf{v}_\perp . Then after collision with the boundary one has:

$$\mathbf{v}'_i = \mathbf{v} - 2\mathbf{v}_\perp + \sqrt{h}\mathbf{f}(t). \quad (3)$$

Particles move in a circular box of radius $R = 1$. A symmetrical container has the advantage that it allows us to examine density and granular temperature gradients along a single coordinate r , the distance from the center of the box, as in the one-dimensional case [7].

We start the simulation by distributing the particles uniformly over the box. When using boundary heating, we give each particle a small, uniformly distributed velocity to enable particles to reach the boundary. Then particles are heated and we allow the system to reach a steady state before taking data. For both uniform heating and boundary heating, data is taken periodically every time step Δt . For uniform heating, data is taken when the particles are heated, so Δt equals the time between heating events.

III. SIMULATION RESULTS: CLUSTERING

If a cluster would develop when heating uniformly it would fall apart very quickly, since every particle is

heated all the time. Things are different for boundary heating. Here, heating only occurs through fast inward-moving particles. Particles in the center of a cluster can be shielded off from heating by particles on the edge of the cluster. As a consequence a stable liquid-like cluster, surrounded by hot gas-like state, will form for certain values of ϕ and η . (Fig. 1) The formation of a cluster spoils measurement of the velocity distribution because the system is no longer in a pure gas-like state. To avoid values of ϕ and η corresponding to the formation of clusters in our simulation, we constructed a phase diagram. We did this by counting for every particle the number N_{6r} of neighbors with their center within a distance $6r$ from that particle. When the gas is in a hexagonal close packed state $N_{6r} = 32$. We obtained the distribution $P(N_{6r})$ for different values of ϕ and η . An example for $N = 350$ and $\phi = 0.1$ is shown in Fig. 2.

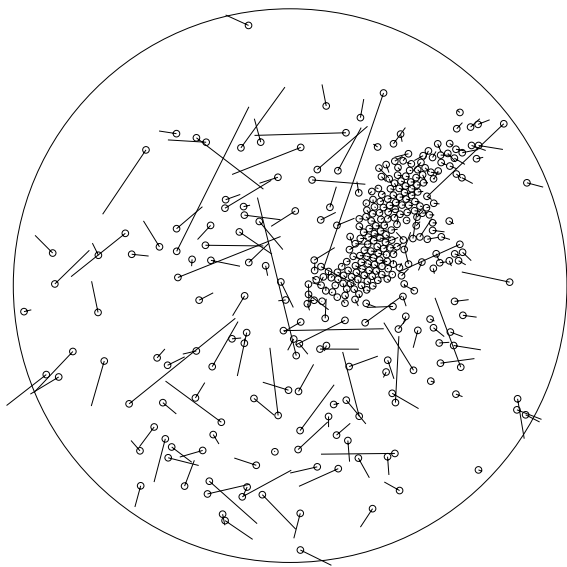


FIG. 1: Snapshot of a clustered state state for $N = 350$, $\phi = 0.05$ and $\eta = 0.6$. The circles indicate the current positions of the particles, while the lines indicate the direction and magnitude of their velocity.

For $\eta = 0.9$ the distribution corresponds to a state with the particles uniformly distributed over the box, with the peak of the distribution at the mean value $\bar{N}_{6r} = 3.6$. For $\eta = 0.7$ the distribution becomes bimodal, with a broad peak at high N_{6r} corresponding to the densely-packed cluster and a peak at $N_{6r} = 1$ corresponding to the surrounding dilute gas. The distribution shows a continuous transition for η in between, which makes it hard to pinpoint an exact value of η for which the gas enters the clustered state. Still, by looking at the shape of the distributions, it can be argued that the transition occurs somewhere between $\eta = 0.75$ and $\eta = 0.85$. This was repeated for different values of ϕ , which allowed us to determine a sort of phase diagram. Specifically, we determined the limit of a pure gas-like phase, and all results presented below were obtained in this state. Because the

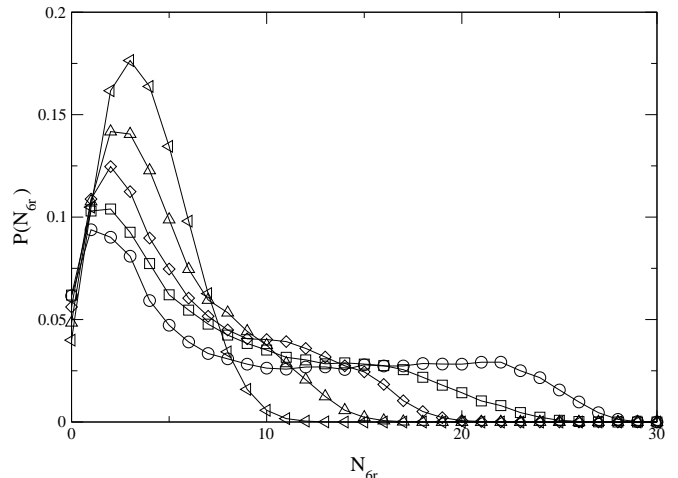


FIG. 2: Number of neighbors within a distance $6r$ of a given particle for $N = 350$, $\phi = 0.1$ and $\eta = 0.7$ (\circ), 0.75 (\square), 0.8 (\diamond), 0.85 (\triangle) and 0.9 (\triangleleft). On average $N_{6r} = 3.6$ for $\phi = 0.1$.

density and kinetic energy are not uniform, there is no sensible thermodynamic limit. Thus, for instance, the appearance of the gas *phase* depends on system size.

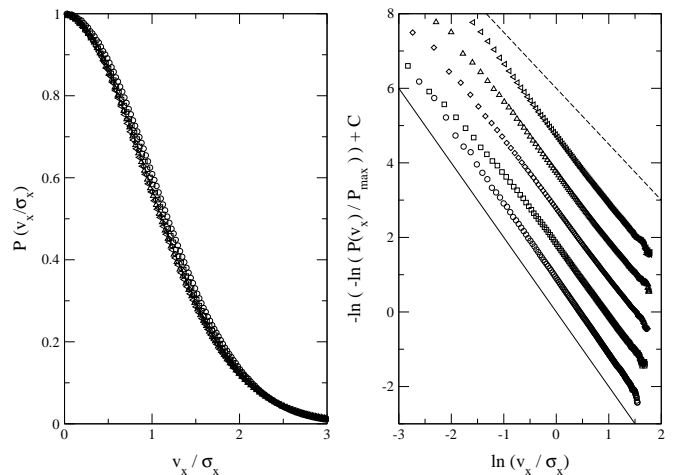


FIG. 3: (a) $P(v_x/\sigma_x)$. (b) $-\ln\{-\ln[P(v_x/\sigma_x)]\}$ versus $\ln(v_x/\sigma_x)$. The dashed lines have slope -2 and -1.5 . Data for both figures is taken for $N = 350$ and for $\phi = 0.02$ and $\eta = 0.8$ (\circ), 0.6 (\square), 0.4 (\diamond), 0.2 (\triangle), 0.1 (\triangleleft).

IV. SIMULATION RESULTS: VELOCITY DISTRIBUTIONS

The velocity distributions $P(v_x)$ for uniform heating are shown in Figs. 3 and 4. The velocity component v_x is scaled by $\sigma_x = \langle v_x^2 \rangle^{1/2}$ and the maximum of the distribution $P(v_x/\sigma_x)$ is scaled to be unity. For a broad range of the parameters ϕ and η the velocity distributions

are very close to Gaussian. For $\eta = 0.8$ the velocity distributions can be fitted by a distribution with $\alpha = 2.0$. This decreases only slightly for $\eta = 0.1$, which can be fitted by a distribution with $\alpha = 1.9$. Values of α are found to be independent of ϕ . These exponents are constant over the entire observed range of velocities and we see no high-velocity tails with $\alpha = 1.5$ for the range of ϕ and η we examined.

For boundary heating the gas develops a gradient in both density and mean kinetic energy as shown in figures 5 and 6. Ideally, we want to measure velocity distributions in a region where the gradient is small. To this end we divided the box in five rings of width 0.2. These rings are indicated in figures 5 and 6. Only for values of ϕ and η close to the clustering state, does the density within a ring vary by more than 10%. The velocity distributions $P(v_x)$ for particles within the different rings are shown in figure 7. Figure 7(a) shows $P(v_x)$ with the velocity component v_x scaled by $\sigma_x = \langle v_x^2 \rangle^{1/2}$ and the maximum of the distribution scaled to be unity. All distributions seem to have the same shape. This is remarkable, since naively one would expect the dynamics of the particles to be different for the different rings. In the center the density is high and particles have many collisions, causing strong spatial correlations. Along the boundary the gas is dilute. Here, many particles have experienced recent collisions with the boundary, and spatial correlations should be much weaker. It has been suggested that these correlations cause the velocity distributions to deviate from Gaussian. But contrary to the expectations, the shape of the distributions seems to be determined by the granular temperature σ_x only. This is a feature that is observed for all values of ϕ and η , even close to the cluster state.

Figure 7(b) shows the behavior of the exponent α . This behavior is very different from the case off uniform heating. For uniform heating α has the same value over the

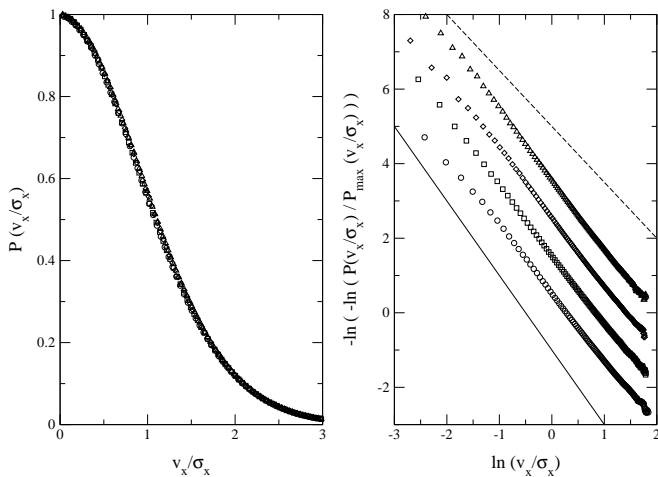


FIG. 4: (a) $P(v_x/\sigma_x)$. (b) $-\ln\{-\ln[P(v_x/\sigma_x)/P_{\max}(v_x/\sigma_x)]\}$ versus $\ln(v_x/\sigma_x)$. The dashed lines have slope -2 and -1.5 . Data for both figures is taken for $N = 350$ and for $\eta = 0.2$ and $\phi = 0.1(\circ)$, $0.05(\square)$, $0.02(\diamond)$, $0.01(\triangle)$.

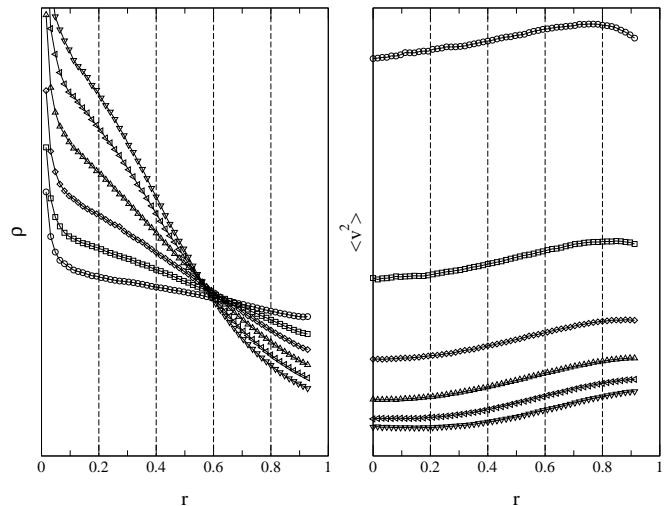


FIG. 5: (a) The average number density ρ as a function of distance r to the center of the box. Data taken for $N = 350$, $\phi = 0.02$ and $\eta = 0.9(\circ)$, $0.8(\square)$, $0.7(\diamond)$, $0.6(\triangle)$, $0.5(\triangleleft)$ and $0.4(\triangleright)$. (b) The mean kinetic energy $\langle v^2 \rangle$ per particle as a function of r , for the same values of ϕ and η . The dashed indicate concentric rings, within which the velocity distributions were separately calculated.

entire observed range of velocities. For boundary heating, on the other hand, α has a constant value α_1 over the low-velocity range but crosses over to different value α_2 when above a critical velocity v_c . For the two innermost rings $\alpha_1 = 1.7$ and $\alpha_2 = 1.0$. For the third ring $\alpha_1 = 1.8$ and the outer ring has $\alpha = 1.5$. For the outer

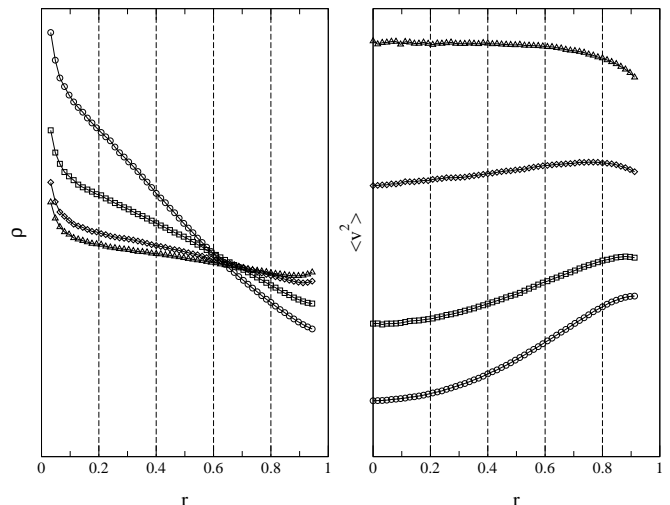


FIG. 6: (a) The average number density ρ as a function of distance r to the center of the box. Data taken for $N = 350$, $\eta = 0.9$ and $\phi = 0.1(\circ)$, $0.05(\square)$, $0.02(\diamond)$ and $0.01(\triangle)$. (b) The mean kinetic energy $\langle v^2 \rangle$ per particle as a function of r , for the same values of ϕ and η .

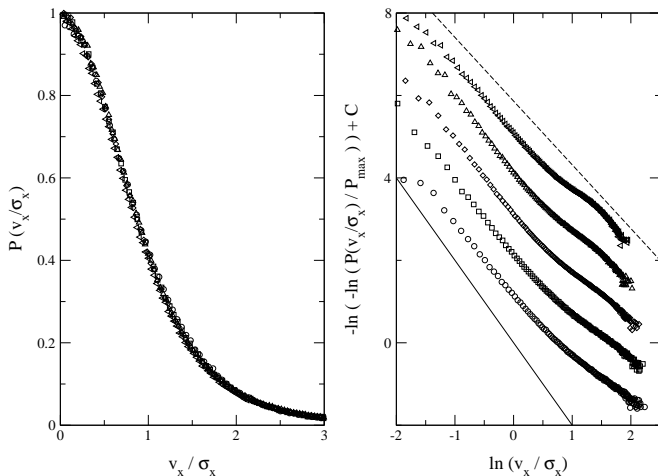


FIG. 7: Velocity distributions calculated separately within the concentric rings shown in Figs. 5 and 6, *i.e.*, for $0 < r \leq 0.2$ (\circ), $0.2 < r \leq 0.4$ (\square), $0.4 < r \leq 0.6$ (\diamond), $0.6 < r \leq 0.8$ (\triangle) and $0.8 < r \leq 1$ (∇), where r is distance to the center. These data were taken for $N = 350$, $\phi = 0.05$ and $\eta = 0.8$. (a) $P(v/\sigma_x)$. (b) $-\ln\{-\ln[P(v_x/\sigma_x)]\}$ versus $\ln(v_x/\sigma_x)$.

two rings the velocity distributions actually undergo two crossovers. First it crosses over to $\alpha_2 \approx 1.0$ and then the exponent increases again to $\alpha_3 \approx 1.5$. In figure 8 we show the effect of a change in ϕ and η on the shape of the velocity distributions. Here we focus on the velocity distribution as measured in the ring with $0.4 < r \leq 0.6$. This has the advantage of good statistics, but for values of ϕ and η close to a cluster, we might see effects due to the density gradient in the gas. As shown in figure 8(a) the exponent $\alpha_1 = 1.8$ except for $\eta = 0.4$, where $\alpha_1 = 1.6$. For $\eta = 0.9$ there is no crossover in the observed range of velocities. In the other distributions one does observe a crossover and the point where it occurs shifts down to lower velocities as η is decreased. It is clear that the distribution for velocities above the crossover cannot be described by a single exponent. For low enough η , the distribution seems to approach a constant exponent for high velocities. This exponent decreases from $\alpha = 1.3$ for $\eta = 0.7$ to $\alpha = 1.0$ for $\eta = 0.4$. In figure 8(b) $\alpha_1 = 1.8$ for $\eta = 0.01$ and $\eta = 0.02$, $\alpha_1 = 1.9$ for $\eta = 0.03$ and $\alpha_1 = 1.7$ for $\eta = 0.05$. For every ϕ does one observe a crossover and the velocity at which the crossover occurs shifts only a bit as ϕ is varied. The distributions approach a constant exponent for high velocities. This exponent goes down from $\alpha = 1.5$ for $\phi = 0.01$ to $\alpha = 1.0$ for $\phi = 0.05$. In general, the deviations from Gaussian become more pronounced as dissipation increases, *i.e.* as ϕ increases or as η decreases.

To test whether the velocity distributions we find here are only observed for this specific driving mechanism of heating through a circular boundary, we constructed different systems that still drive in an inhomogeneous way. For instance, we constructed a box with periodic boundary conditions that includes a small circular region

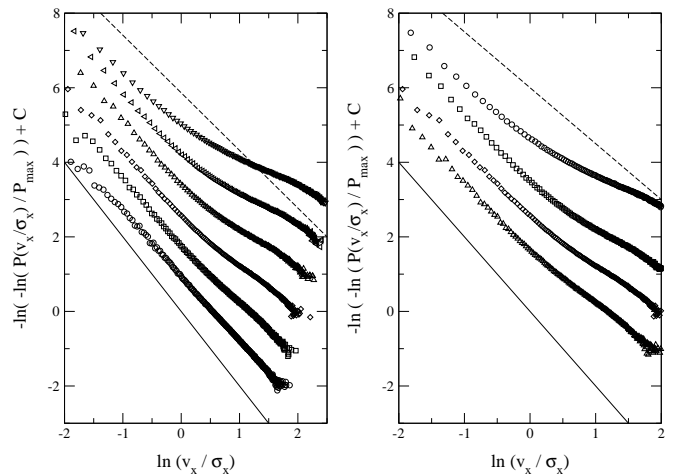


FIG. 8: (a) $-\ln\{-\ln[P(v_x/\sigma_x)]\}$ versus $\ln(v_x/\sigma_x)$ for $N = 350$, $\phi = 0.02$ and $\eta = 0.9$ (\circ), 0.8 (\square), 0.7 (\diamond), 0.6 (\triangle), 0.5 (∇) and 0.4 (∇). (b) $-\ln\{-\ln[P(v_x/\sigma_x)]\}$ versus $\ln(v_x/\sigma_x)$ for $N = 350$, $\eta = 0.7$ and $\phi = 0.01$ (\circ), 0.02 (\square), 0.03 (\diamond) and 0.05 (\triangle).

around the center. Within this circular region particles are uniformly driven but outside of it they are not heated at all. For particles within the circular region we observe velocity distributions with an exponent constant over the whole range as in uniform heating. On the other hand, for particles outside of the circular region we observe the same velocity distributions as seen in boundary heating. This suggests that the velocity distributions described here are general to inhomogeneous heating.

For uniform heating the distribution of velocities of particles that are heated is gaussian, because the velocities undergo a random walk. This is not the case for the particles heated at the boundary. To see if velocity distributions are sensitive to the precise way of heating at the boundary, we changed our heating algorithm so that, when a particle hits a boundary, it's new velocity is drawn from a gaussian distribution. This has a modest effect on the far end of the high-velocity tail, but leaves all major differences between uniform and boundary heating intact.

Finally, we studied the behavior of the velocity distribution for different particle numbers N . Figure 9(a) shows that, as N increases, the velocity distributions fall off more rapidly, but the high-velocity tails grow longer. This is shown more clearly in figure 9(b). For $N = 100$ the exponent $\alpha_1 = 1.5$, but for $N = 1000$ it increases to $\alpha_1 = 2.0$. For the high-velocity tail, on the other hand, one has $\alpha_2 = 1.7$ for $N = 100$ decreasing to $\alpha_2 = 0.7$ for $N = 1000$. The crossover shifts to lower velocity and becomes sharper as N is increased. Rouyer and Memon worked with particle number $100 < N < 500$ [8]. Figure 9 shows that in this regime distributions suffer from finite-size effects. Still, the crossover persists to higher particle numbers, suggesting this to be a general feature of boundary heating.

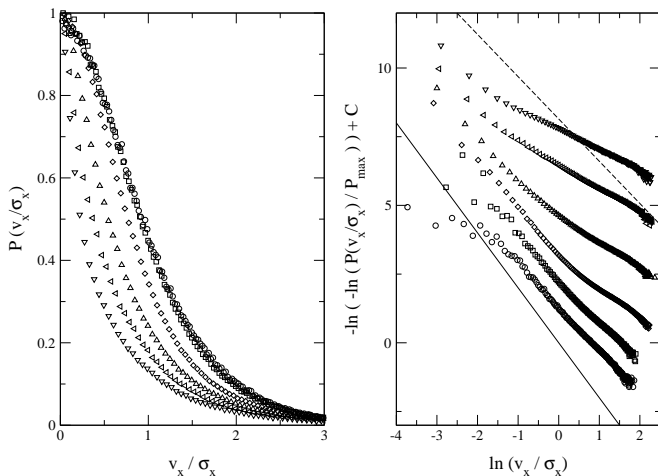


FIG. 9: (a) $P(v_x/\sigma_x)$ for different values of N . (b) $-\ln\{-\ln[P(v_x/\sigma_x)]\}$ versus $\ln(v_x/\sigma_x)$. Data is taken for $\phi = 0.05$, $\eta = 0.8$ and $N = 100(\circ)$, $200(\square)$, $500(\diamond)$, $700(\Delta)$ and $1000(\triangleleft)$.

For their experiments Rouer and Menon used N particles with $\eta \approx 0.9$, where $100 < N < 500$ and $0.05 < \phi < 0.25$ [8]. In figure 10 we plotted the velocity distribution for $\eta = 0.9$, $\phi = 0.05$ and several values of N . We also indicated in grey the fit with $\alpha = 1.52$ as made in [8]. This line clearly coincides with the high-velocity tail of the velocity distribution found by simulation. This suggests

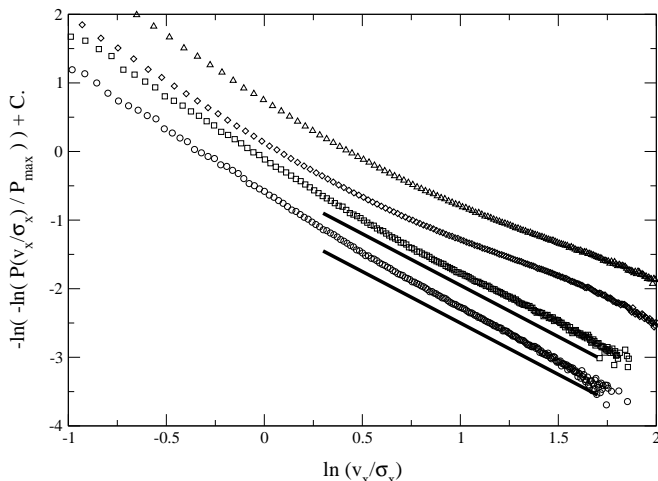


FIG. 10: (a) $-\ln\{-\ln[P(v_x/\sigma_x)]\}$ versus $\ln(v_x/\sigma_x)$ for $N = 350$, $\phi = 0.05$ and $\eta = 0.9$ (\circ), $N = 500$, $\phi = 0.05$ and $\eta = 0.9$ (\square), $N = 350$, $\phi = 0.05$ and $\eta = 0.8$ (\diamond), $N = 350$, $\phi = 0.25$ and $\eta = 0.9$ (Δ). The solid lines correspond to the fit as made by Rouyer and Menon and has an exponent $\alpha = 1.52$. The range of the solid lines corresponds to half the range used by Rouyer and Menon in their fit, but contains about 80% of their data points

that it is very well possible that instead of a universal distribution with $\alpha = 1.5$, they only observed a part of a more complex velocity distribution, with two exponents and a crossover. For higher ϕ the high-velocity tails have exponents that are smaller than the $\alpha = 1.5$ observed for $\phi = 0.05$

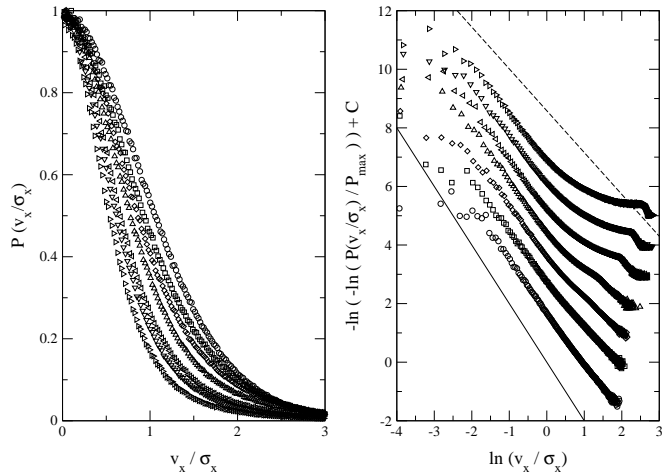


FIG. 11: (a) $P(v_x/\sigma_x)$ for different values of Δt . (b) $-\ln\{-\ln[P(v_x/\sigma_x)]\}$ versus $\ln(v_x/\sigma_x)$. Data is taken for $N = 350$, $\phi = 0.02$, $\eta = 0.4$ and $\Delta t = 0.01(\circ)$, $0.03(\square)$, $0.05(\diamond)$, $0.10(\Delta)$, $0.30(\triangleleft)$, $0.50(\nabla)$ and $1.00(\triangleright)$.

A possible explanation for the occurrence of a crossover in the velocity distribution for boundary heating might be found in a system studied by Moon et. al. [4]. They study a uniformly driven gas, but nevertheless find velocity distributions with a clear crossover. The main difference is the way they implement uniform heating. Every time Δt , they select at random two particles and add to these particles a random but opposite velocity to conserve the total momentum. On average heating is spatially homogeneous and in the limit of very small Δt the behavior of both their and our uniform heating algorithm is the same. For small enough Δt the number of collisions between heating events is smaller than one and the heating dominates over the dissipative behavior of the gas. When Δt becomes larger, many collisions might happen between two heating events. This allows the gas to cool down between heating events and this seriously alters the velocity distributions. In figure 11 we show the velocity distribution for $N = 350$, $\phi = 0.02$ and $\eta = 0.4$. The gas is heated using the two-point heating algorithm described above and we varied Δt . For $\Delta t = 0.01$ the distribution has a exponent $\alpha = 1.7$ that is constant over the observed range. When Δt is reduced a clear crossover develops. The behavior of the velocity distribution for velocities higher than the crossover velocity is more complicated than in boundary heating. There is also a sharp kink at the high-velocity end, although particles are heated in a gaussian way.

It is very well possible that the considerations above also apply to the velocity distributions we found for uni-

form and boundary heating. When heating uniformly all the particles are heated every timestep Δt , while only a few collisions occur in that time. The system is dominated by heating and we see a velocity distribution with a constant exponent over the entire observed velocity range. If we are heating through a boundary, there are many collisions in the dense region in the center of the box, but only a few particles escape to the boundary to get heated. In this case, the system is dominated by dissipation and we see in general a velocity distribution that strongly deviates from a Gaussian. This difference between uniform and boundary heating can be quantified by the fraction $f = \overline{N}_h / \overline{N}_c$, where \overline{N}_h and \overline{N}_c are an average over a certain amount of time of the number of heatings and the number of collisions a particle has suffered, respectively. For a uniformly heated gas of $N = 350$, $\phi = 0.02$ and $\eta = 0.4$ we find that $f = 120$. For the same parameters but heating through the boundary we find $f = 0.08$. For again the same parameters but using two-point heating with $\Delta t = 1.0$ we find $f = 0.012$.

V. A SIMPLE MODEL WITHOUT SPATIAL DEGREES OF FREEDOM

To study the dependence of the velocity distributions on the fraction f we constructed a model of the inelastic gas inspired by work done by Ulam [12] on elastic gases. Ulam rederived the Maxwell-Boltzmann distribution for the velocities of particles in a perfect gas using the following very simple model: he considered N particles with random initial velocities. At every time step a pair of particles was selected and the velocities of the particles were changed as if they had collided elastically. Ulam found that, regardless of the initial velocities, the system quickly evolved to a state where on average all energy was distributed equally over all particles and the deviation of the velocities of the particles around the average velocity of the system was given by the Maxwell-Boltzmann distribution. This approximation of random collisions is only justified when the gas is sufficiently dilute. The same approximation can also be made for the granular gas by replacing the elastic collisions between particles with inelastic collisions. Since the gas cools down without any further energy input, heating has to be included as well. This allows us to study the dissipative behavior of the granular gas while neglecting all spatial correlations that develop in the more detailed simulations described before. In particular we can study the effect on the velocity distributions of changing the fraction $f = \overline{N}_h / \overline{N}_c$ described in the previous chapter by varying the ratio of heatings and collisions.

We adapted Ulam's procedure in order to model a two-dimensional granular gas consisting of N particles. Equa-

tion 1 can be cast into the following form:

$$\mathbf{v}'_i = \mathbf{v}_i - \frac{1 + \eta}{2} \begin{pmatrix} \cos^2 \theta & \sin \theta \cos \theta \\ \sin \theta \cos \theta & \sin^2 \theta \end{pmatrix} (\mathbf{v}_i - \mathbf{v}_j), \quad (4)$$

where \mathbf{v}_i and \mathbf{v}_j are the velocities of particles i and j , η is the coefficient of restitution and θ is the angle between the separation vector \mathbf{r}_{ij} and a reference axis. Collisions in our model occur by selecting at random particles i and j and an uniformly distributed impact parameter $-2R < b < 2R$. We then use the above collision rule with $\theta = \arcsin(b/2R) + \arccos(\mathbf{v} \cdot \hat{\mathbf{s}}/v)$, where $\mathbf{v} = (\mathbf{v}_j - \mathbf{v}_i)/2$ is the velocity in the center-of-mass frame and $\hat{\mathbf{s}}$ is a unit vector along the reference axis. We discard values of θ corresponding to $(\mathbf{v}_j - \mathbf{v}_i) \cdot \mathbf{r}_{ij} < 0$ as these represent unphysical collisions. We heat the gas by selecting a random particle i and adding a random amount of velocity according to equation 2. To prevent the velocities from running away, we subtract the center-of-mass velocity after heating. In a single time step, we have C collisions and we heat H particles. This gives us $f = \frac{H}{2C}$.

When we use inelastic instead of elastic collisions and drive the system, we find that the gas heats up until it reaches a steady state, where on average the energy lost in collisions is compensated by the heat inserted into the system through our driving mechanism. As C is chosen increasingly bigger in comparison to H , the granular temperature σ of the gas decreases accordingly.

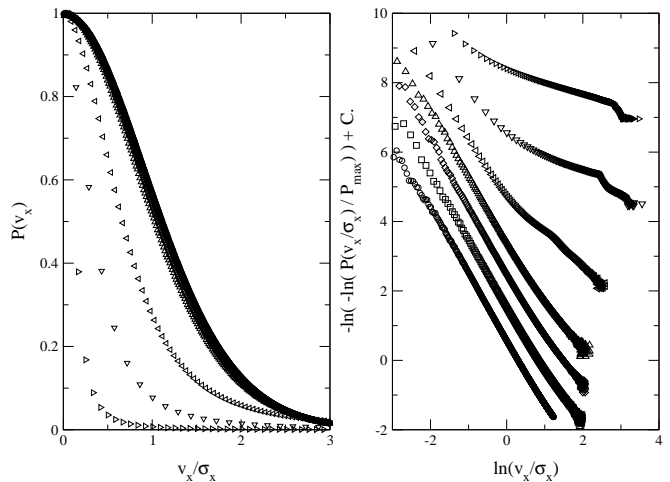


FIG. 12: Velocity distribution for an inelastic gas of $N = 500$ and $\eta = 0.4$. (a) $P(v_x/\sigma_x)$. (b) $-\ln\{-\ln[P(v_x/\sigma_x)]\}$ versus $\ln(v_x/\sigma_x)$. Data is for different values of $f = \frac{H}{2C}$: $f = 50$ (\circ), $f = 5$ (\square), $f = 1$ (\diamond), $f = 0.5$ (\triangle), $f = 0.05$ (\triangleleft), $f = 5 \cdot 10^{-3}$ (∇) and $f = 5 \cdot 10^{-4}$ (\triangleright).

In figure 12 we plotted the result for an inelastic gas with $\eta = 0.4$. We varied the number of heatings and the number of collisions in a single time step from $H = 100$ and $C = 1$ to $H = 1$ and $C = 1000$. As f is lowered, the

velocity distributions develop a crossover and for $f \ll 1$ there also appears an irregular kink at the high-velocity tail. The velocity distributions for $f \ll 1$ are reminiscent of the distributions seen in two-point heating for comparable f . The kink we see for $\Delta t \geq 0.30$ in two-point heating might even be a part of the more complicated kink we see at $f = 5 \cdot 10^{-3}$. For $f = 50$ the distribution has an exponent $\alpha = 2.0$. This reduces to $\alpha = 1.9$ for $f = 0.5$. After the crossover the exponent is $\alpha = 1.3$. For $f = 0.05$ the exponent has reduced to $\alpha = 1.7$ and the distribution shows complicated behavior after the crossover. This is more extreme for $f = 5 \cdot 10^{-3}$. In figure 13 we keep $f = 0.025$ fixed and vary η . We see that the crossover point shifts down as η is lowered and that the kink in the velocity distribution shifts down.

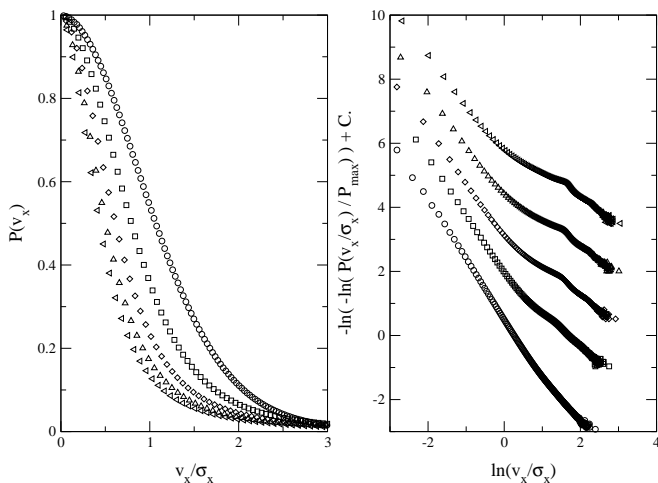


FIG. 13: Velocity distribution for an inelastic gas of $N = 500$ and $f = 0.025$. (a) $P(v_x/\sigma_x)$. (b) $-\ln\{-\ln[P(v_x/\sigma_x)]\}$ versus $\ln(v_x/\sigma_x)$. Data is for $\eta = 0.9$ (o), 0.7 (\square), 0.5 (\diamond), 0.3 (\triangle) and 0.1 (\triangleleft).

We also compared velocity distributions found in the model with those acquired by simulation. To this end we measured f in simulations using different ways of heating. For a uniformly heated gas of $N = 350$, $\phi = 0.02$ and $\eta = 0.4$ we found $f = 120$. For the same parameters but heating through the boundary we found $f = 0.08$. For two-point heating with $\Delta t = 1.0$ we found $f = 0.012$. We ran the model with the corresponding set of parameters and measured velocity distributions. The results are shown in figure 14.

The velocity distributions agree qualitatively, but especially for the case of $f=0.08$ there is considerable quantitative difference. This might be due to the fact that the gas is not dilute enough to justify the random collision approximation. Still, the model is able to generate non-Gaussian velocity distributions, while neglecting all spatial correlations. This suggests that the non-Gaussian behavior of the velocity distributions is not caused by spatial fluctuations and correlations in the gas. Instead

it is the flow of energy through the system, mediated by the inelastic collisions, that determines the shape of the velocity distribution. This also means that there is no a priori difference between inhomogeneous and homogeneous heating: the difference in the shape of the velocity distribution, particularly the occurrence of the crossover, is only a consequence of the fact that in inhomogeneous heating in general the number of collisions between particles exceeds the number of particles being heated.

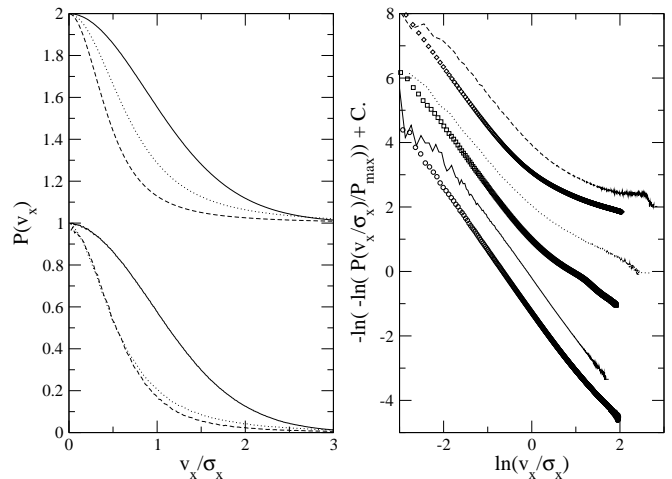


FIG. 14: Velocity distributions for an inelastic gas of $N = 500$ and $\eta = 0.4$. (a) $P(v_x/\sigma_x)$ for $f = 120$ (solid), $f = 0.08$ (dashed) and $f = 0.012$ (dotted). Results on the bottom are obtained for simulation, results on the top for the model. (b) $-\ln\{-\ln[P(v_x/\sigma_x)]\}$ versus $\ln(v_x/\sigma_x)$. The symbols shown are velocity distributions acquired by simulation for $f = 120$ (solid), $f = 0.08$ (dashed) and $f = 0.012$ (dotted). (\diamond). The lines show the velocity distributions found in the model for $f = 120$ (o), 0.08 (\square), 0.012.

VI. CONCLUSION

We compared the velocity distributions of a granular gas that was heated in a spatially homogeneous way, by uniform heating, and in a spatially inhomogeneous way, by heating through the boundary. Although it is usually assumed that uniform heating yields the same behavior as boundary heating when the boundary is far away and the spatial gradients are small, we find that there are clear qualitative differences. When driven through the boundary, for instance, the gas can form coexisting cool liquid-like clusters surrounded by a hot gaseous state for certain values of ϕ and η . Such clusters have no equivalent in uniform heating.

The difference between uniform heating and boundary heating also extends to the velocity distributions. For uniform heating, we find velocity distributions that are close to Gaussian over the observed range of velocities

and for a wide range of ϕ and η . When heating through the boundaries, on the other hand, we find that velocity distributions usually cross over from one exponent to another. For the high-velocity tail we find that the exponent varies over a wide range. For strongly dissipative systems this tail may not be described by a single exponent. The velocity distributions do not depend on the precise way of heating: the behavior appears to be general to inhomogeneous heating, as was checked using different heating mechanisms.

This means that there is no universal velocity distribution with $\alpha = 1.5$, as was proposed by Rouyer and Menon. Instead, the velocity distribution found by Rouyer and Menon may be just one out of the many distributions described here. The apparent universality may be due to the use of a narrow range of parameters (nearly elastic particles were used with $\eta = 0.93$ and vary $0.05 \leq \phi \leq 0.25$). We find that varying ϕ only has a less pronounced effect on the shape of the distribution when η is so close to the elastic limit. For low η , we instead find velocity distributions that look much like the distributions found by Blair and Kudrolli for gases with $\eta \approx 0.5$.

Furthermore, we find that when using two-point heating, we can change the behavior of the velocity distributions by varying the time between heating events. When the number of collisions between heating events is very small, we find velocity distributions like those observed in uniform heating. As the number of collisions increases, we observe velocity distributions reminiscent of boundary heating. As the number of collisions is increased even further we observe extremely non-Gaussian velocity distributions that fall off very slowly for high velocities and ultimately show a sharp kink at the high-velocity end. We introduced the fraction $f = \overline{N}_H / \overline{N}_C$, where \overline{N}_H is number of times a particle is heated on average and \overline{N}_C is the number of times a particle undergoes a collision

on average. In two-point heating we observe velocity distribution reminiscent of uniform heating for a value of f that is of the same order as the value of f measured directly in a uniformly heated gas and we find velocity distributions like the distributions found in boundary heating for a value of f that is comparable to the value of f as measured directly in a gas heated through the boundary.

Very similar results were reproduced in a simple model that approximates a very dilute granular gas, but which ignores spatial degrees of freedom. Here, we find velocity distributions ranging from nearly Gaussian to strongly non-Gaussian, when varying f from $f \gg 1$, where dissipation is dominated by heating, to $f \ll 1$, where dissipation dominates the heating. Again we find velocity distributions with the same characteristics as those found in uniform or boundary heating, only when f is of the same order as the value for f measured directly in uniform or boundary heating. Although there is qualitative agreement between the results of the model and the simulations, they do not agree qualitatively. Still, since there is no spatial information in our model, we suggest that the velocity distributions are non-Gaussian not because of spatial correlations or density fluctuations, but rather because of the way energy is injected and redistributed over the other particles through inelastic collisions. More specifically, it is the cascade of energy from a few high-energy particles to the slow-moving particles in the bulk of the gas that seems to be the key determinant of the non-Gaussian velocity distributions.

The results of two-point heating and the above model, suggest that particularly in the dilute case, where the influence of the spatial correlations is small, the velocity distributions we find might be special cases of a universal velocity distribution, after all. This universal velocity distribution might not be described by the parameters ϕ and η , but by f and η instead. More work will be needed to establish this.

-
- [1] S. McNamara, W.R. Young, Phys. Rev. E 50, R28 (1994)
 - [2] T. Zhou, L.P. Kadanoff, Phys. Rev. E 54, 623 (1996)
 - [3] D.R.M. Williams, F.C. MacKintosh, Phys. Rev. E, 54, R9
 - [4] S.J. Moon, M.D. Shattuck, J.B. Swift, Phys. Rev. E 64, 031303 (2001)
 - [5] T.P.C. van Noije, M.H. Ernst, Granular Matter 1, 57 (1998)
 - [6] S. Luding, E. Clément, A. Blumen, J. Raichenbach, J. Duran, Phys. Rev. E 49, 1634 (1994)
 - [7] Y.S. Du, H. Li, L.P. Kadanoff, Phys. Rev. Lett. 74, 1268 (1995)
 - [8] F. Rouyer, N. Menon, Phys. Rev. Lett. 85, 3676 (2000)
 - [9] A. Samadani, A. Kudrolli, Phys. Rev. E 64, 051301 (2001)
 - [10] J.S. Olafsen and J.S. Urbach, Phys. Rev. E 60, R2468 (1999)
 - [11] A. Puglisi, V. Loreto, U. M. B. Marconi, A. Petri and A. Vulpiani, Phys. Rev. Lett 81, 3848 (1998)
 - [12] S. Ulam, Adv. Appl. Math. 1, 7 (1980)